

# Rejecting Heave-induced Pressure Oscillations in a Semilinear Hyperbolic Well Model

Timm Strecker<sup>1</sup> and Ole Morten Aamo<sup>1</sup>

**Abstract**—In this paper, we apply recent results on the output feedback control of  $2 \times 2$  semilinear systems to the problem of rejecting heave-induced pressure oscillations in offshore drilling. The well is modeled as a transmission line with nonlinear friction, with both actuation and measurement restricted to one boundary. The heave motion is represented by disturbance terms entering both inside the domain and at the uncontrolled boundary. We construct an output feedback controller to track a reference pressure at one location in the well. The controller performance is demonstrated in simulations.

## I. INTRODUCTION

Several interesting problems in the drilling industry involve the control of distributed parameter systems [1]. During drilling, a well is filled with a fluid called mud. In order to avoid undesired outflow of the mud into the surrounding formation, influx of formation fluids into the well, or even collapse of the well, it is essential to keep the mud pressure within predefined margins. In managed pressure drilling (MPD), the top of the well is sealed such that the pressure and mud flow at the top of the well can be controlled via a choke and a backpressure pump [2]. However, vertical movement of the drill string causes surge and swab pressures that can violate the pressure margins [3]. In particular, we are concerned with the case that the drill string motion is caused by heave. Heave is the wave-induced vertical motion of a floating offshore rig. While so-called heave compensators decouple the drill string from the rig's motion during drilling, every approximately 30 m the drill string needs to be rigidly attached to the heaving rig in order to extend the drill string by a new segment. In this paper, we consider the problem of rejecting heave-induced pressure oscillations using the topside choke for actuation and measurements that are available on the rig. This problem has been considered in several papers, using a range of control methods for finite dimensional systems [4], [5], [6]. More relevant to the present study is [7], in which results from [8] were exploited to develop a backstepping controller to track a reference pressure at the bottom of the well. The heave motion is modeled as harmonic oscillations affecting the boundary, and the controller achieves exact tracking of the reference pressure if disturbance predictions are correct. In [9], this approach was generalized to reject disturbances at an arbitrary point in the domain, and the result was applied to the heave problem in [10]. In [11], a

model where the disturbance also enters inside the domain was considered. In these papers, the well is modeled by linear  $2 \times 2$  hyperbolic partial differential equations (PDEs). However, a linear model cannot be expected to be accurate in many cases, because commonly used rheology models of drilling muds, such as the Herschel Bulkley model [12], are highly nonlinear at low shear rates. In [13], we demonstrated that nonlinear friction in such muds has a significant effect on heave-induced pressure oscillations. There, we also presented a parameter fitting procedure to obtain explicit friction terms for Herschel Bulkley fluids. Introducing the nonlinear friction terms into the well model, the model becomes semilinear. Recently, we developed an output-feedback controller for this class of systems [14]. In the present paper, we demonstrate how this control method is applied to reject disturbances in the semilinear well model.

The remainder of the paper is organized as follows. The governing equations and the problem statement are given in Section II. In Section III, we present recent results on controller and observer design for  $2 \times 2$  semilinear hyperbolic systems. The practical application of these methods is presented in Section IV. In Section V, the controller performance is demonstrated in several simulations, before concluding remarks are given in Section VI.

## II. MODELING

We assume that the drill string is rigid, which is a reasonable assumption during heave in approximately vertical wells up to 5000 m depth. A well is basically a long, thin fluid-filled conduit. In [15], [16], a variety of transmission line models for such cases are presented. In this paper, we use the following model for the pressure and flow rate in the well, which was also used in [7], [10], [11] except for the different friction term:

$$p_t(z, t) = -\frac{\beta}{A} q_z(z, t) \quad (1)$$

$$q_t(z, t) = -\frac{A}{\rho} p_z(z, t) - \frac{1}{\rho} F(q(z, t), v_d(t)) - Ag \quad (2)$$

$$q(0, t) = -A_d v_d(t) \quad (3)$$

where  $z \in [0, l]$  is the position measured from the bottom,  $t \geq 0$  is time,  $l$  is the length of the well,  $p(z, t)$  is pressure,  $q(z, t)$  the volumetric flow rate, the subscripts  $z$  and  $t$  denote partial derivatives with respect to space and time, respectively,  $v_d(t)$  is the drill string velocity,  $A$  the cross sectional area of the annulus,  $A_d$  is the area displaced by the drill string,  $\beta$  is the bulk modulus,  $\rho$  the density, and  $g$  the gravitational acceleration.  $F$  is a nonlinear function representing friction,

\*This work was supported by Statoil ASA

<sup>1</sup>The authors are with the Department of Engineering Cybernetics, Norwegian University of Science and Technology (NTNU), Trondheim N-7491, Norway (e-mail: timm.strecker@itk.ntnu.no, aamo@ntnu.no)

and is constructed as described in [13] for a given mud rheology and well geometry. The parameters  $A$ ,  $\beta$ ,  $\rho$ , and  $F$  can vary with  $z$ , but since it would change nothing but notation we omit this dependence for the sake of readability. The control objective is to control the pressure at  $\bar{z} \in [0, l]$  to a given setpoint  $p_{sp}$ , i.e.

$$p(\bar{z}, t) = p_{sp}. \quad (4)$$

The topside boundary condition can be controlled via the choke and the backpressure pump, and is left as the control input. Moreover, we assume that both the topside pressure and flow rate,  $p(l, t)$  and  $q(l, t)$ , can be measured.

#### A. Heave

The controller that we use in this paper requires short term predictions of  $v_d$ . This will be made precise in Section III-A. The time pressure waves take to propagate from the choke to  $\bar{z}$ , i.e. the delay between topside actuation and its effect at the location of the control objective, is in the same range as the wave period. This makes the prediction of the disturbance critical for the controller performance. To obtain short term predictions of the disturbance, we model the heave as harmonic oscillations, i.e.

$$\dot{X}(t) = \bar{A}X(t), \quad (5)$$

$$v_d(t) = \bar{C}X(t), \quad (6)$$

where

$$\bar{A} = \text{diag} \left( \begin{bmatrix} 0 & \omega_1 \\ -\omega_1 & 0 \end{bmatrix}, \dots, \begin{bmatrix} 0 & \omega_n \\ -\omega_n & 0 \end{bmatrix} \right), \quad (7)$$

$$\bar{C} = [0 \quad 1 \quad \dots \quad 0 \quad 1] \quad (8)$$

for  $n$  distinct frequencies  $\omega_1, \dots, \omega_n$ . We assume that  $v_d$  equals the rig's vertical velocity, and assume that measurements  $y(t)$  of the rig velocity are available. In practice,  $y$  could for instance be estimated using an accelerometer combined with an observer. Thus,  $X(t)$  can be estimated from  $y(t)$  using the observer

$$\hat{X}(t) = \bar{A}\hat{X}(t) + L(y(t) - \hat{y}(t)), \quad (9)$$

$$\hat{y}(t) = \bar{C}\hat{X}(t), \quad (10)$$

where the observer gain  $L$  is chosen such that  $\bar{A} - L\bar{C}$  is Hurwitz.

#### B. State Transformation

Hyperbolic PDEs simplify to ODEs along their characteristic lines, making the method of characteristic a powerful and popular tool for the analysis of hyperbolic systems. Therefore, we transform the system into diagonal form, and also rescale the domain into the unit interval  $[0, 1]$ . The transformation

$$u(x, t) = \frac{1}{2} \left( q(lx, t) + \frac{A}{\sqrt{\beta\rho}} (p(lx, t) - p_{sp} + \rho g(lx - \bar{z})) \right), \quad (11)$$

$$v(x, t) = \frac{1}{2} \left( q(lx, t) - \frac{A}{\sqrt{\beta\rho}} (p(lx, t) - p_{sp} + \rho g(lx - \bar{z})) \right), \quad (12)$$

maps (1)-(3) into

$$u_t(x, t) = -\varepsilon_u(x)u_x(x, t) + F_u(u(x, t), v(x, t), v_d(t)), \quad (13)$$

$$v_t(x, t) = \varepsilon_v(x)v_x(x, t) + F_v(u(x, t), v(x, t), v_d(t)), \quad (14)$$

$$u(0, t) = -v(0, t) + d(t), \quad (15)$$

$$v(1, t) = U(t), \quad (16)$$

$$Y(t) = u(1, t), \quad (17)$$

where  $x \in [0, 1]$  and

$$\varepsilon_u(x) = \varepsilon_v(x) = \frac{1}{l} \sqrt{\frac{\beta}{\rho}}, \quad d(t) = -A_d v_d(t), \quad (18)$$

$$F_u(u, v, v_d) = F_v(u, v, v_d) = -\frac{1}{2\rho} F(u + v, v_d). \quad (19)$$

The control objective becomes

$$u(\bar{x}, t) = v(\bar{x}, t) \quad (20)$$

for  $\bar{x} = \bar{z}/l$ .  $U$  is the actuation. In terms of the original physical system, we have

$$U(t) = \frac{1}{2} \left( q(l, t) - \frac{A}{\sqrt{\beta\rho}} (p(l, t) - p_{sp} + \rho g(l - \bar{z})) \right). \quad (21)$$

In practice, the actuation  $U(t)$  cannot be implemented directly but must be realized by controlling the opening of the choke. Briefly speaking, closing the choke decreases  $q(l, t)$  and increases  $p(l, t)$ , hence decreases  $U(t)$ . Analogously, opening the choke increases  $U(t)$ . In the remainder of this paper, we assume that a sufficiently fast choke controller is implemented such that  $U(t)$  as given by (21) tracks the desired actuation, and treat  $U(t)$  as the actuation.  $Y(t)$  is the measurements, which in terms of physical quantities equals

$$Y(t) = \frac{1}{2} \left( q(l, t) + \frac{A}{\sqrt{\beta\rho}} (p(l, t) - p_{sp} + \rho g(l - \bar{z})) \right). \quad (22)$$

### III. EXACT CONTROL AND STATE ESTIMATION

The transformed system (13)-(17) has the structure of the general  $2 \times 2$  semilinear hyperbolic system in [14]. The controller and observer design method from [14], which we apply to the heave model in this paper, exploits the system dynamics on the characteristic lines. For this purpose, it is necessary to define the characteristic lines  $s_v(\cdot, t)$  along which the actuation  $U(t)$  evolves, and the characteristic lines  $s_u(\cdot, t)$  along which the measurement  $Y(t)$  evolves. They are given by

$$\phi_v(x) = \int_x^1 \frac{1}{\varepsilon_v(\xi)} d\xi, \quad \phi_u(x) = \int_x^1 \frac{1}{\varepsilon_u(\xi)} d\xi, \quad (23)$$

$$\tau_v(x, t) = t + \phi_v(x), \quad \tau_u(x, t) = t - \phi_u(x), \quad (24)$$

$$s_v(x, t) = (x, \tau_v(x, t)) \quad s_u(x, t) = (x, \tau_u(x, t)). \quad (25)$$

$s_u$  and  $s_v$  are also depicted as the wider lines in Figure 1. As opposed to the quasilinear case, the characteristic lines are known a priori in semilinear systems. Moreover, we define the states on  $s_v$  and  $s_u$  as

$$\tilde{u}(x, t) = u(x, \tau_v(x, t)), \quad \tilde{v}(x, t) = v(x, \tau_v(x, t)), \quad (26)$$

$$\check{u}(x, t) = u(x, \tau_u(x, t)), \quad \check{v}(x, t) = v(x, \tau_u(x, t)). \quad (27)$$

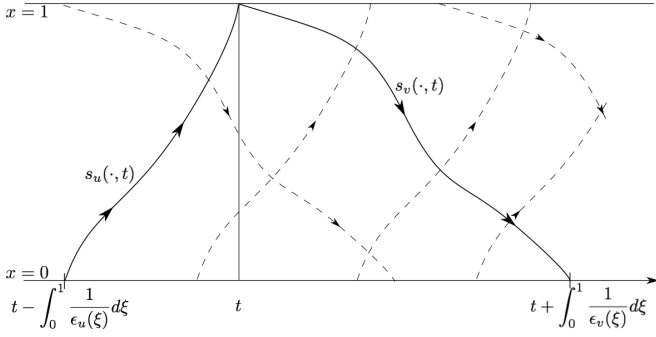


Fig. 1. Characteristic lines of  $u$  ("upwards") and  $v$  ("downwards").

### A. State Feedback Controller

The control input  $U(t)$  propagates from  $x = 1$  to  $x = 0$  with finite speed  $\varepsilon_v$  along the characteristic line  $s_v(\cdot, t)$ . Roughly speaking, the control input  $U(t)$  affects only the state  $v(x, \tau_v(x, t)) = \tilde{v}(x, t)$  for  $x \in [0, 1]$  before reaching the boundary  $x = 0$ . The states  $v(x, \theta)$  for  $x \in [0, 1]$  and  $\theta < \tau_v(x, t)$ , and  $u(x, \theta)$  for  $x \in (0, 1]$  and  $\theta \leq \tau_v(x, t)$ , are entirely determined by the state at time  $t$ ,  $(u(\cdot, t), v(\cdot, t))$ , and the disturbance term  $v_d$  up to time  $\tau_v(x, t)$ . This was made precise in [14], where it was shown that for every  $t$ , there exists a continuous operator  $\Phi^t$ , independent of  $U(t)$ , such that

$$\tilde{u}(\cdot, t) = \Phi^t(u(\cdot, t), v(\cdot, t)). \quad (28)$$

*Remark 1:* When evaluated at time  $t$ , the operator  $\Phi^t$  involves values of  $F_u$  and  $F_v$ , and thus of  $v_d$ , in the time interval  $[t, \tau_v(0, t)]$ . While this is fine from a mathematical perspective, it means that  $\Phi^t$  is non causal. The practical implementation of  $\Phi^t$  will be discussed in Section IV.

Since  $v(\bar{x}, \theta)$  for  $\theta \in [t, \tau_v(\bar{x}, t)]$  is entirely determined by the state at time  $t$ , we can use  $U(t)$  only to control  $v(\bar{x}, \tau_v(\bar{x}, t))$ , i.e.  $v$  at  $\bar{x} = \phi_v(\bar{x})$  into the future. We denote the desired  $v(\bar{x}, \tau_v(\bar{x}, t))$  by  $U^*(t)$ , and design  $U(t)$  such that  $v(\bar{x}, \tau_v(\bar{x}, t))$  tracks  $U^*(t)$ . Assuming that at time  $t$ , the disturbance  $v_d$  is known up to time  $\tau_v(\bar{x}, t)$ , it is possible to determine  $U^*(t)$  by evaluating the objective (20) at time  $\tau_v(\bar{x}, t)$  using the prediction  $\tilde{u}(\cdot, t)$  of  $u$ , i.e.

$$U^*(t) = u(\bar{x}, \tau_v(\bar{x}, t)) = \tilde{u}(\bar{x}, t). \quad (29)$$

If  $\bar{x} \in (0, 1]$ ,  $\tilde{u}(\bar{x}, t)$  is given by  $\Phi^t(u(\cdot, t), v(\cdot, t))$ . If  $\bar{x} = 0$ ,  $\tilde{u}(0, t)$  is determined by (15), i.e.

$$\tilde{u}(0, t) = -\tilde{v}(0, t) + d(\tau_v(0, t)) = -U^*(t) - A_d v_d(\tau_v(0, t)). \quad (30)$$

Inserting (30) into (29) and solving for  $U^*(t)$  yields

$$U^*(t) = \frac{1}{2}d(t + \phi_v(0)). \quad (31)$$

Finally,  $U(t)$  is constructed by solving the dynamics of  $\tilde{v}(\cdot, t)$  along  $s_v(\cdot, t)$  backwards in time. In [14], it was shown that  $\tilde{v}(\cdot, t)$  satisfies the ODE

$$\tilde{v}_x(x, t) = -\frac{1}{\varepsilon_v(x)}F_v(\tilde{u}(x, t), \tilde{v}(x, t), v_d(\tau_v(x, t))) \quad (32)$$

with  $\tilde{v}(1, t) = U(t)$ . The goal is to design  $U(t)$  such that the solution of (32) satisfies  $\tilde{v}(\bar{x}, t) = U^*(t)$ . Thus,  $U(t)$  can be obtained as  $U(t) = \varphi(1)$ , where  $\varphi$  is the solution of the Cauchy problem

$$\varphi_x(x) = -\frac{1}{\varepsilon_v(x)}F_v(\tilde{u}(x, t), \varphi(x), v_d(\tau_v(x, t))), \quad \varphi(\bar{x}) = U^*(t), \quad (33)$$

in the domain  $x \in [\bar{x}, 1]$ . With this design,  $(\tilde{u}, \tilde{v})$  satisfies  $\tilde{v}(\bar{x}, t) = U^*(t)$ , i.e. the tracking objective (20), for all  $t \geq 0$ . Hence, by definition (26),  $(u, v)$  satisfies (20) for all  $t \geq \phi_v(\bar{x})$ .

### B. Observer

The measurement  $Y(t)$  evolved along the characteristic line  $s_u(\cdot, t)$ . Loosely speaking, the state at some location  $x$  and time  $\theta > \tau_u(x, t)$  has no influence on  $Y(t)$ . Moreover, the state at time  $t$ ,  $(u(\cdot, t), v(\cdot, t))$ , is entirely determined by the past state on  $s_u(\cdot, t)$ ,  $(\tilde{u}(\cdot, t), \tilde{v}(\cdot, t))$ . More precisely, it was proven in [14] that for every  $t$ , there exists a continuous operator  $\Lambda^t$ , independent of  $U(t)$ , such that

$$(u(\cdot, t), v(\cdot, t)) = \Lambda^t(\tilde{u}(\cdot, t), \tilde{v}(\cdot, t)). \quad (34)$$

We repeat here the observer from [14]

$$\hat{u}_x(x, t) = \frac{1}{\varepsilon_u(x)}F_u(\hat{u}(x, t), \hat{v}(x, t), v_d(\tau_u(x, t))), \quad (35)$$

$$\hat{v}_t(x, t) = \frac{\varepsilon_u(x)\varepsilon_v(x)}{\varepsilon_u(x) + \varepsilon_v(x)}\hat{v}_x(x, t) + \frac{\varepsilon_u(x)}{\varepsilon_u(x) + \varepsilon_v(x)}F_v(\hat{u}(x, t), \hat{v}(x, t), v_d(\tau_u(x, t))), \quad (36)$$

$$\hat{v}(x, 0) = \hat{v}_0(x), \quad (37)$$

$$\hat{u}(1, t) = Y(t), \quad (38)$$

$$\hat{v}(1, t) = U(t), \quad (39)$$

for some initial guess  $\hat{v}_0 \in L^\infty([0, 1])$ . (35)-(39) is a copy of the dynamics of  $(\tilde{u}, \tilde{v})$  with the boundary condition at  $x = 0$ , which would have been  $\tilde{u}(0, t) = -\tilde{v}(0, t) + d(\tau_u(0, t))$ , replaced by the measurement (38). Exchanging these is possible because (35) is an ODE in space without any dynamics in time. As shown in [14], the observer errors  $\tilde{u} - \hat{u}$  and  $\tilde{v} - \hat{v}$  become zero within

$$t_o = \phi_v(0) + \phi_v(0). \quad (40)$$

Thus,

$$(u(\cdot, t), v(\cdot, t)) = \Lambda^t(\hat{u}(\cdot, t), \hat{v}(\cdot, t)) \quad (41)$$

for all  $t \geq t_o$ .

*Remark 2:* When evaluated at time  $t$ , the operator  $\Lambda^t$  involves values of  $F_u$  and  $F_v$ , and thus of  $v_d$ , in the past time interval  $[\tau_u(\bar{x}, t), t]$ . Thus,  $\Lambda^t$  is causal. Likewise, the observer (35)-(39) is causal.

## IV. APPLICATION TO WELL MODEL

We apply the output feedback controller consisting of the transformation (11)-(12), the state-feedback controller from Section III-A and the observer from Section III-B to system (1)-(3). However, in this form the state feedback control law is not causal because it uses future values of

the disturbance as stated in Remark 1. In order to obtain a causal feedback law, we replace the future disturbance terms by their prediction. Using the heave model (5)-(6) and the estimate  $\hat{X}$  obtained from the observer (9)-(10), a prediction of  $v_d$  that is available at time  $t$  is given by

$$\bar{v}_d^t(\theta) = \bar{C}e^{\bar{A}(\theta-t)}\hat{X}(t) \quad (42)$$

for  $\theta \geq t$ . In the following, we denote all variables that use the prediction instead of the true future value by a bar and a superscript  $t$  to indicate the time at which the prediction is made, i.e.  $\bar{d}^t(\theta) = -A_d\bar{v}_d^t(\theta)$ , and similarly  $\bar{F}_u^t$ ,  $\bar{F}_v^t$ , and  $\bar{\Phi}^t$ . Note that the observer (35)-(39) and  $\Lambda^t$  are causal, as stated in Remark 2.

Summarizing, evaluating the output-feedback controller at time  $t$  consists of the the following steps

- 1) measure  $Y(t)$  as given in (22).
- 2) using the current estimator state  $\hat{v}(\cdot, t)$ , determine  $\hat{u}(\cdot, t)$  via (35) with (38).
- 3) determine the current estimated state via

$$(u_{est}(\cdot, t), v_{est}(\cdot, t)) = \Lambda^t(\hat{u}(\cdot, t), \hat{v}(\cdot, t)). \quad (43)$$

The  $\Lambda^t$ -operator is implemented by solving the PDE system (13)-(15) in the domain  $\{(x, \theta) : x \in [0, 1], \theta \in [\tau_u(x, t), t]\}$  with 'initial condition'  $v(x, \tau_u(x, t)) = \hat{v}(x, t)$  for  $x \in [0, 1]$ .

- 4) using the state  $\hat{X}$  of the heave observer (9)-(10), construct the heave prediction  $\bar{v}_d^t$  as stated in (42).
- 5) determine the predicted state  $\bar{u}(\cdot, t)$  via

$$\bar{u}(\cdot, t) = \bar{\Phi}^t(u_{est}(\cdot, t), v_{est}(\cdot, t)). \quad (44)$$

The  $\bar{\Phi}^t$ -operator is implemented by solving the PDE system (13)-(15) in the domain  $\{(x, \theta) : x \in [0, 1], \theta \in [t, \tau_v(x, t)]\}$  with initial condition  $(u_{est}(\cdot, t), v_{est}(\cdot, t))$ , using the prediction  $\bar{v}_d^t$  instead of the true  $v_d$ .

- 6) determine  $\bar{U}^*(t)$  as  $\bar{U}^*(t) = \bar{u}(\bar{x}, t)$  if  $\bar{x} \in (0, 1]$ , or  $\bar{U}^*(t) = \frac{1}{2}\bar{d}^t(t + \phi_v(0))$  if  $\bar{x} = 0$ .
- 7) determine  $U(t)$  by solving the Cauchy problem

$$\varphi_x(x) = -\frac{1}{\varepsilon_v(x)}F_v(\bar{u}(x, t), \varphi(x), \bar{v}_d^t(\tau_v(x, t))) \quad (45)$$

with initial condition  $\varphi(\bar{x}) = \bar{U}^*(t)$  in the domain  $x \in [\bar{x}, 1]$ , and setting  $U(t) = \varphi(1)$ .

- 8) apply  $U(t)$  as given in (21).
- 9) update  $\hat{v}$  according to (36) with (39), and  $\hat{X}$  according to (9).

## V. SIMULATIONS

We consider a 3000 m deep vertical well with 216 mm diameter and 127 mm drill string outer diameter, hence  $A = 0.0239 \text{ m}^2$  and  $A_d = 0.0127 \text{ m}^2$ . The mud has density  $1500 \text{ kg/m}^3$ , bulk modulus 16000 bar, and a Bingham-type rheology with plastic viscosity 20 mPas and yield point 5 Pa. With this rheology and well geometry, the parameter fitting procedure from [13] returns the following friction term:

$$F(q, v_d) = \sum_{i=1}^2 \left( c_0^i + c_K^i |v_{eff}^i|^{n^i} \right) s(v_{eff}^i), \quad (46)$$

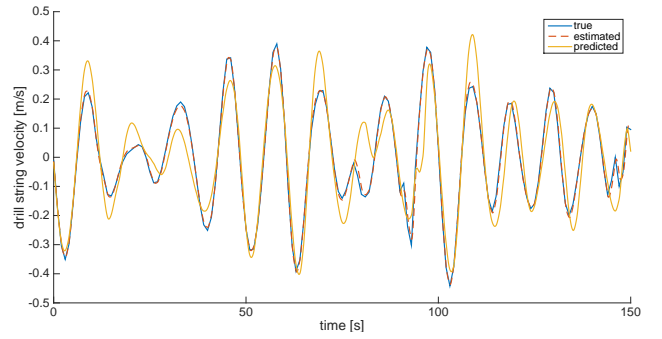


Fig. 2. Heave velocity.

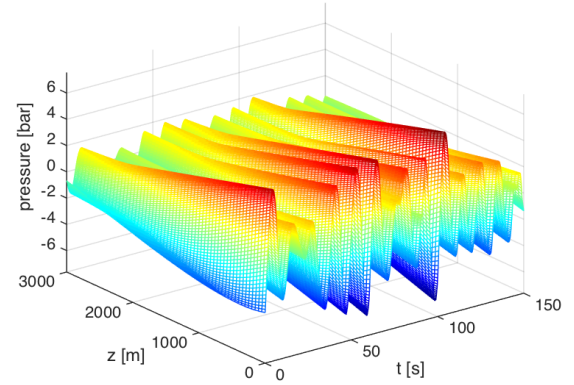


Fig. 3. Pressure deviation from steady state using  $U(t) = 0$ .

where  $v_{eff}^i = q/A - k^i v_d$ ,

$$c_0^1 = 2, \quad c_K^1 = 2, \quad n^1 = 1, \quad k^1 = 0.8, \quad (47)$$

$$c_0^2 = 3.4, \quad c_K^2 = 3, \quad n^2 = 0.95, \quad k^2 = 0.07, \quad (48)$$

and

$$s(v) = \frac{v}{\sqrt{v^2 + 0.01}} \quad (49)$$

is a smooth approximation of the sign function.

We use heave data measured on a rig as input to the simulations. The time series of the rig velocity, as well as the estimated velocity using the observer (9)-(10) and the predicted velocity according to (42),  $\bar{v}_d^{t-\phi_v(0)}(t)$ , with prediction time  $\phi_v(0) \approx 3 \text{ s}$ , is depicted in Figure 2. The amplitude of the corresponding heave motion is approximately 0.8 m. While the estimation lies almost exactly on the measurement, the stochasticity of the waves causes errors in the predicted velocity.

The pressure for the uncontrolled case (using  $U(t) = 0 \forall t$ ) is depicted in Figure 3.  $U(t) = 0$  corresponds approximately to a constant choke opening. The heave causes pressure oscillations in the magnitude of  $\pm 5 \text{ bar}$  at the bottom of the well. Due to friction, the pressure amplitudes decreases significantly with the distance form the bottom.

### A. Pressure Control at the Bottom of the Well

The pressure trajectory when using the output-feedback controller to track the reference pressure  $p_{sp} = 460 \text{ bar}$  at

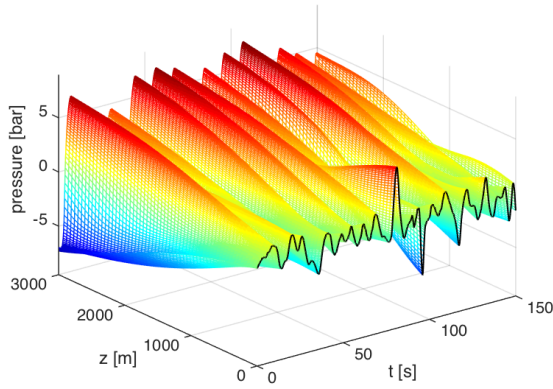


Fig. 4. Pressure deviation from steady state using the output feedback controller for  $\bar{z} = 0$ .

the bottom of the well, i.e. at  $\bar{z} = 0$ , is depicted in Figure 4. The pressure oscillations at the bottom of the well are also depicted in Figure 5. The controller succeeds in reducing the pressure oscillations at the bottom of the well. However, there are significant downhole pressure fluctuations at times when the wave prediction is inaccurate, which occasionally are in the same range as the pressure oscillations without control. For comparison, the bottomhole pressure when using the non causal controller that has access to exact wave predictions is also depicted. The pressure is almost exactly on the setpoint, with small pressure errors due to numerical inaccuracies. This illustrates how the stochasticity of the heave induces limitations on the achievable controller performance. Relative large pressures are required at the topside choke in order to overcome friction along the well. The choke pressure (Figure 6) needs to be changed accurately by several bar within a few seconds, which might be a challenge in practice. Moreover, the required control actuation increases in drilling muds with higher viscosity.

In Figure 7, the relative estimation errors for the transformed variables  $u$  and  $v$  are depicted. The corresponding estimation error in the pressure is in the range of  $\pm 0.5$  bar. These errors are due to numerical inaccuracies in the implementation of the observer (35)-(39) and  $\Lambda^l$ . The steep curvature of  $F$  around zero velocities ( $F$  involves a slightly smoothed sign function, see also (46)) makes the numerical implementation challenging.

### B. Pressure Control in the Interior

The pressure trajectory when tracking the reference pressure  $p_{sp} = 310$  bar at  $\bar{z} = 1000$ , i.e. 1000 m above the bottom of the well, is depicted in Figure 8. This case is of interest, for instance, when the area around the so-called casing shoe is the most sensitive part of the well. The pressure time series at  $\bar{z}$  and at the choke are depicted in Figures 9 and 10. The controller rejects the the pressure oscillations accurately, and more efficiently than for  $\bar{z} = 0$ . This is simply because the prediction time  $\phi_v(\bar{x})$  is shorter for  $\bar{x} = \frac{1}{3}$  than for  $\bar{x} = 0$ , making the heave prediction more accurate.

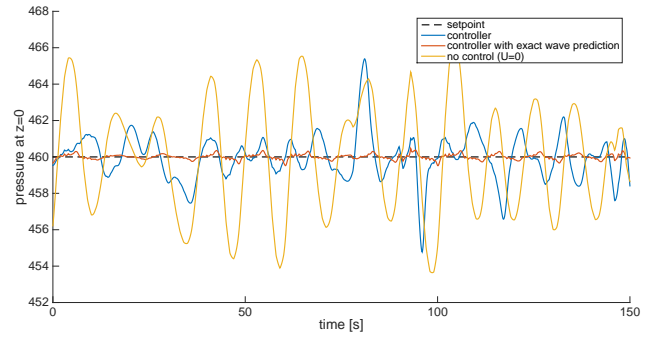


Fig. 5. Pressure at the bottom of the well using the output feedback controller, the (non causal) controller with exact wave predictions, and  $U = 0$ .

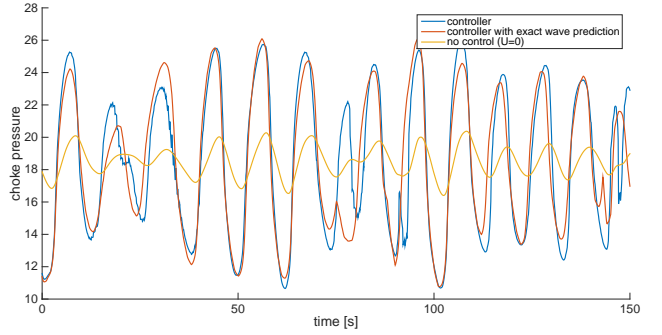


Fig. 6. Pressure at the topside choke.

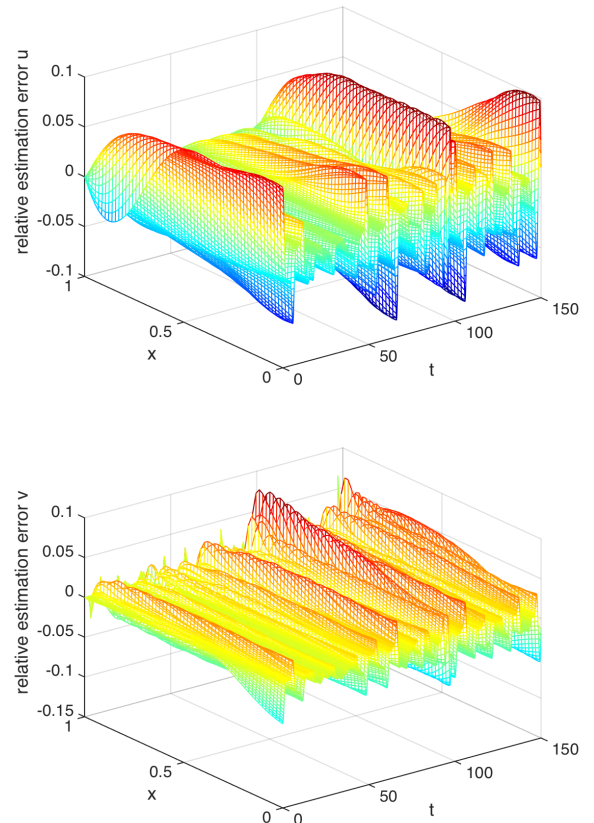


Fig. 7. Relative estimation errors  $(u - u_{est})/\|u\|_\infty$  and  $(v - v_{est})/\|v\|_\infty$ .

## VI. CONCLUSIONS

We applied a recently developed output feedback controller to reject disturbances in an oil well modeled by a system of  $2 \times 2$  semilinear hyperbolic PDEs. The practical implementation of the controller was discussed. Simulations demonstrate that the controller can effectively reject pressure oscillations. However, limitations on the achievable performance exist due to errors in the heave prediction, and because the control law can reject pressure oscillations only at one location in the well. These limitations are inherent to the physics of the problem if only the actuation and measurements as in this paper are used. In future work, the sensitivity with respect to modeling errors should be investigated. Moreover, the controller design method should be extended to include the drill string elasticity.

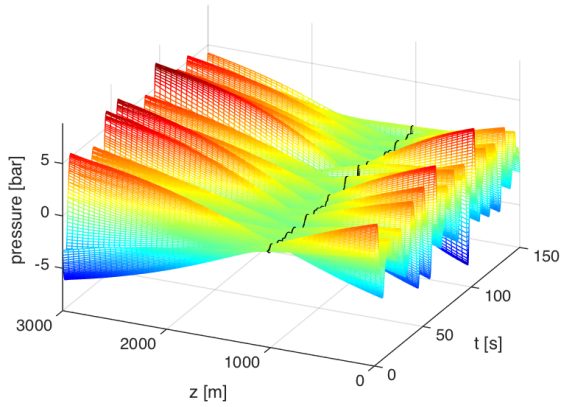


Fig. 8. Pressure deviation from steady state using the output feedback controller for  $\bar{z} = 1000$ .

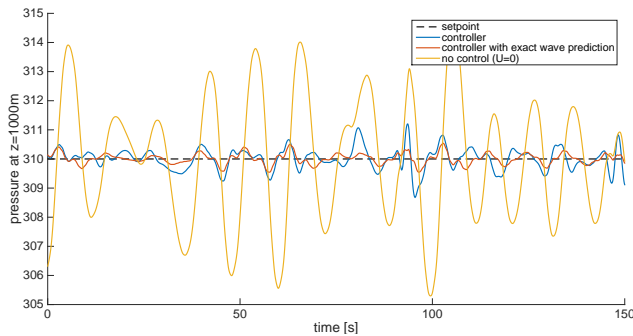


Fig. 9. Pressure at  $\bar{z} = 1000$ .

This can also be seen in Figure 10, where the actuation using the prediction-based and the non causal controller with exact wave prediction are very close. Figure 8 demonstrates another limit on the achievable controller performance: In practice, it is usually desirable to reject pressure oscillations in a section of the well, rather than at just one location. However, as seen in Figure 8, even if the pressure oscillations are rejected effectively at one location, significant pressure oscillations occur within a few hundred meters of  $\bar{z}$ .

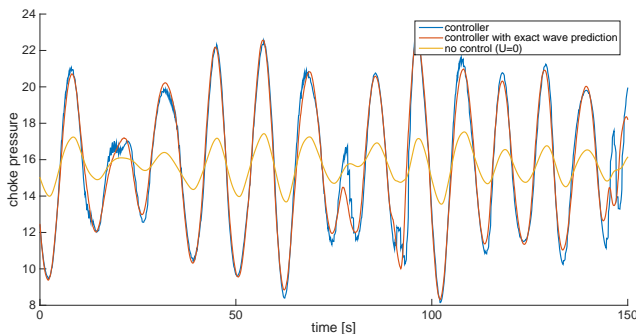


Fig. 10. Choke pressure for  $\bar{z} = 1000$ .

## REFERENCES

- [1] F. Di Meglio and U. Aarsnes, "A distributed parameter systems view of control problems in drilling," in *2nd IFAC Workshop on Automatic Control in Offshore Oil and Gas Production, Florianópolis, Brazil*, 2015.
- [2] J.-M. Godhavn *et al.*, "Control requirements for automatic managed pressure drilling system," *SPE Drilling & Completion*, vol. 25, no. 03, pp. 336–345, 2010.
- [3] R. Mitchell, "Dynamic surge/swab pressure predictions," *SPE drilling engineering*, vol. 3, no. 03, pp. 325–333, 1988.
- [4] I. S. Landet, A. Pavlov, and O. M. Aamo, "Modeling and control of heave-induced pressure fluctuations in managed pressure drilling," *IEEE Transactions on Control Systems Technology*, vol. 21, no. 4, pp. 1340–1351, 2013.
- [5] A. Albert, O. M. Aamo, J.-M. Godhavn, and A. Pavlov, "Suppressing pressure oscillations in offshore drilling: Control design and experimental results," *IEEE Transactions on Control Systems Technology*, vol. 23, no. 2, pp. 813–819, 2015.
- [6] H. Mahdianfar, N. Hovakimyan, A. Pavlov, and O. M. Aamo, "L 1 adaptive output regulator design with application to managed pressure drilling," *Journal of Process Control*, vol. 42, pp. 1–13, 2016.
- [7] O. M. Aamo, "Disturbance rejection in  $2 \times 2$  linear hyperbolic systems," *IEEE Transactions on Automatic Control*, vol. 58, no. 5, pp. 1095–1106, 2013.
- [8] R. Vazquez, M. Krstic, and J.-M. Coron, "Backstepping boundary stabilization and state estimation of a  $2 \times 2$  linear hyperbolic system," in *2011 50th IEEE Conference on Decision and Control and European Control Conference (CDC-ECC)*, 2011, pp. 4937–4942.
- [9] H. Anfinsen and O. M. Aamo, "Disturbance rejection in the interior domain of linear  $2 \times 2$  hyperbolic systems," *IEEE Transactions on Automatic Control*, vol. 60, no. 1, pp. 186–191, 2015.
- [10] —, "Rejection of heave-induced pressure fluctuations at the casing shoe in managed pressure drilling," *IFAC Proceedings Volumes*, vol. 47, no. 3, pp. 7717–7722, 2014.
- [11] T. Strecker and O. M. Aamo, "Rejecting pressure fluctuations induced by string movement in drilling," in *2nd IFAC Workshop on Control of Systems Governed by Partial Differential Equation*, 2016.
- [12] R. API RP 13D, "Rheology and hydraulics of oil-well drilling fluids," 2006.
- [13] T. Strecker and O. M. Aamo, "Simulation of heave-induced pressure oscillations in herschel-bulkley muds," *accepted for publication in SPE Journal*, 2017.
- [14] —, "Output feedback control of  $2 \times 2$  semilinear hyperbolic systems," *submitted to Automatica*, 2016.
- [15] J. Stecki and D. Davis, "Fluid transmission lines-distributed parameter models part 1: A review of the state of the art," *Proceedings of the Institution of Mechanical Engineers, Part A: Journal of Power and Energy*, vol. 200, no. 4, pp. 215–228, 1986.
- [16] —, "Fluid transmission lines-distributed parameter models part 2: comparison of models," *Proceedings of the Institution of Mechanical Engineers, Part A: Journal of Power and Energy*, vol. 200, no. 4, pp. 229–236, 1986.